

## **STEEL CASING OVERHEATING ANALYSIS OF OPERATING POWER PIPE-TYPE CABLES**

F. P. Dawalibi, J. Liu, S. Fortin, S. Tee, and Y. Yang  
Safe Engineering Services & technologies ltd.  
1544 Viel, Montreal, Quebec, Canada  
Email: info@sestech.com; Web Site: www.sestech.com

### **ABSTRACT**

This paper discusses the analysis of an overheating problem which has been observed within a 140' (43 m) long steel pipe casing containing 115 kV three-phase electric power cables. A steel casing electromagnetic field model has been built to determine the induced current (eddy currents) distribution along the radial, transverse, and longitudinal directions of the casing caused by the energized cables under different operating conditions. This model takes the combined effects of the inductive, conductive, and capacitive interference into account. This study involved a circuit model to determine the voltage and current distributions in the conductors of the buried power cables. Furthermore, a detailed analytical model of the cylindrical steel casing (assuming an infinitely long casing) was conducted to determine the actual paths of eddy current flow and their density throughout the cross section from the inner surface to the outer surface of the steel casing. The computation results show that induced currents in the steel casing can cause significant heat losses and that the exact distribution of the induced current density within the steel casing plays a crucial role in the heat losses generated by such currents.

### **KEY WORDS**

Electromagnetic fields, pipe-type cable, steel casing, overheating, eddy currents, and power system operation

### **1. Introduction**

With the continuous increase in the capacity of power systems, the overheating problem of steel casings containing pipe-type power cables is becoming more serious and requires more attention. The heat loss associated with currents flowing in power cables installed inside steel pipes is the result of induced currents (eddy currents) within the pipe wall due to the electromagnetic fields generated by the current flow.

This paper describes a real case that resulted in significant overheating within a 140' (43 m) long steel pipe casing containing 115 kV three-phase electric power cables. The problem was serious enough that the derating of the power cables had to be considered. The primary objective of this paper is to determine if the electromagnetic fields

generated by the power cables inside the steel casing can induce eddy currents in the steel casing that will result in overheating effects within the steel casing everywhere or at some specific spots along its length.

Several methods were used concurrently in order to insure that the investigation analysis is accurate and that any analysis result is credible. The first step involved modeling the underground power cable circuit network to determine the voltage and current distributions in the cables. This model accounted for the cross-bonding of the cable sheaths and armors. In the next step, electromagnetic field models of the steel casing were built to determine the induced current distributions along the radial, transverse, and longitudinal directions of the casing based on the current distributions among the power cables from the results computed using the circuit model. The third step of the analysis was to build a complete analytical model [1-2] of the cylindrical steel casing (assuming an infinitely long casing). This effort was made to cross-validate the results obtained in the first two steps and to obtain a preliminary estimate of the eddy current losses based on actual current densities in the steel casing rather than average values which were obtained from the electromagnetic field models.

This paper focuses on the second step and presents an analysis based on electromagnetic field theory. By solving Maxwell's electromagnetic field equations, it takes induction effects fully into account. The computation results contain the combined effects of the inductive, conductive, and capacitive interference.

The computation results provide the precise locations and densities of the currents within the casing, including end effects, proximity effects, and skin depth effects.

### **2. Description of Overheating Problem**

#### **2.1. Overall System Configuration**

The overall system configuration is shown in Figure 1. Substation 2 feeds two 115 kV underground circuits that terminate at Substation 1. Most of the circuits are underground except at the substation take-offs where the underground cables emerge at the overhead termination

structure. The overall length of the buried cables is 4552' (1387 m). There are two manholes located at 1540' (469 m) and 3140' (957 m) from Substation 2. A 140' (43 m) long steel pipe casing contains 115 kV three-phase electric power cables. The casing is buried at a depth of 36" (0.9 m) in the earth.

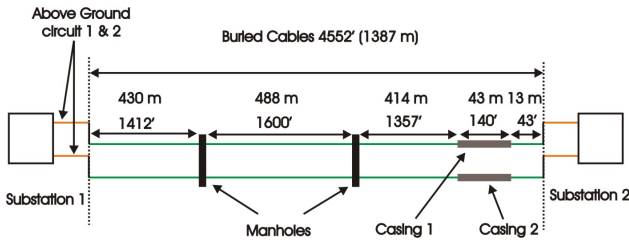


Figure 1. Plan View of the Electric Network

2.2. Parameters of Pipe-Type Power Cables

The cables consist of a stranded conductor core surrounded by an aluminum sheath and a lead sheath all separated or covered by insulating material. The 115 kV cable core is a 3000 kcmil copper conductor. The aluminum sheath is made of dense wires that were approximated as a tubular 80 mils thick conductor. The tubular lead sheath (armor) is 82 mils thick. All other layers are assumed to be made of a perfect insulating material.

The positions of the power cables and the cross sections of the steel casings are shown in Figure 2. The power cables are buried inside a typical bore spacer steel casing. The internal medium of the casing is concrete with a resistivity of 100 ohm-m. Two circuits are installed along with an insulated grounding conductor. However, only one circuit was operational when the overheating problem was observed.

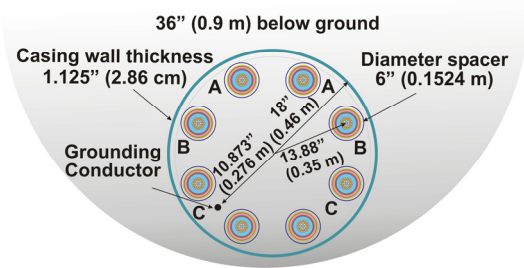


Figure 2. Power Cables and Casing Cross Section

3. Circuit Model Results

A circuit model of the power system network was developed using TRALIN™ and SPLITS™, the line parameter and current distribution analysis software modules of the CDEGS® package [3] to determine voltages and load currents, including current unbalances within the power cables and associated shields, armors,

and casings. The following operating conditions were studied:

- Normal load (500 A) and emergency load (1390 A at a power factor of 0.95) and operating conditions on the energized phase conductors.
- One arrangement assumed no cross-bonding between sheaths and armors. All cable sheaths, armors and the insulated neutral conductors are connected at the manhole sections to a 20 ohm ground. The other arrangement assumed that the sheaths and armors were cross-bonded at each manhole location.

The results under the emergency load conditions are shown in Table 1. Note that the cable current is the residual current, i.e., the sum of the core, sheath, and armor currents.

Table 1. Scenarios Examined Using the Circuit Model for Emergency Load Conditions

Scenario Analyzed	Sheath & Armor Cross-Bonding	Energized Cables and Conductors	Active Current (A)	Reactive Current (A)
1 (Casing 1)	No	Cable A	18.22568	-415.316
		Cable B	311.7019	376.4676
		Cable C	-347.108	-33.2849
		Ground Conductor	-2.85284	24.42758
2 (Casing 2)	No	Cable A	13.95004	-409.681
		Cable B	307.2706	379.4617
		Cable C	-364.761	-32.0478
		Ground Conductor	41.08006	1.457637
3 (Casing 1)	Yes	Cable A	1394.846	-3.62568
		Cable B	-674.561	1141.538
		Cable C	-563.553	-1164.14
		Ground Conductor	-106.56	-54.0293
4 (Casing 2)	Yes	Cable A	1374.796	-40.1326
		Cable B	-696.437	1103.229
		Cable C	-588.19	-1211.2
		Ground Conductor	46.8291	141.691

4. Electromagnetic Field Analysis

In the electromagnetic field model, the steel casing and power cables as well as the insulated grounding conductor were modeled. The power cables were modeled as equivalent conductors. The steel casing was assumed to be immersed in a 100 ohm-m soil. The main objective of this electromagnetic field analysis was to determine the nature of the currents that are induced in the steel casing by the currents flowing in the power cables located inside the casing. An approximate three dimensional mesh model of the casing was built using HIFREQ™ the electromagnetic software engineering module of the CDEGS® package [3, 4]. The analysis was conducted in various steps that introduced progressively the final computer model. The intermediate models were initially

developed to determine the extent of the induced current distribution along the main three dimensions of the model (i.e., radial, transversal, and longitudinal directions of the steel casing, see Figure 3). The computation results revealed that the radial component of the induced currents is not significant. It is only 4% of the induced longitudinal or transversal currents and can be neglected. Furthermore, the induced longitudinal (axial) currents were found to be practically constant along the casing except near the ends. The transverse or circular induced currents reached their highest levels near the ends of the casing and then dropped rapidly within a few feet to negligible levels.

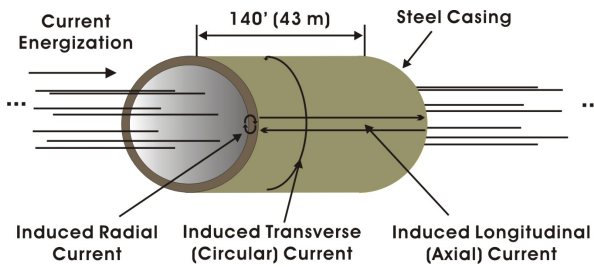


Figure 3. Steel Casing Induced Current Distributions

Based on the intermediate computation results, the final computer model of the steel casing was simplified as described in Section 4.1.

**4.1. Enhanced Electromagnetic Field Model**

The steel casing and power cable electromagnetic field model is shown in Figure 4.

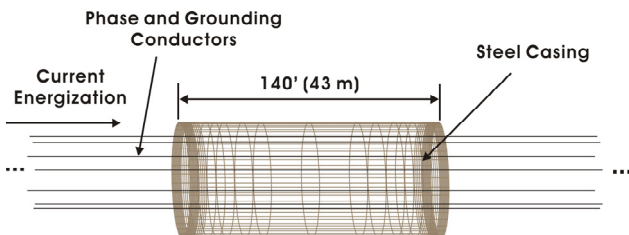


Figure 4. Equivalent Model of the Steel Casing Including Energized Conductors (Power Cables)

The cross section of the cylindrical steel casing was modeled as a polygon of 40 sides as shown in Figure 5.

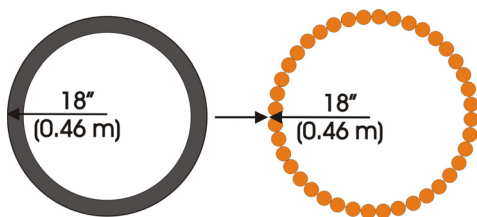


Figure 5. Wires along the Transverse (Circular) Direction of the Casing

The actual casing wall thickness is 1.125” (2.86 cm). The diameter of the wires is selected in such a way that the

longitudinal area covered by the wires equals the casing cross-section area. Therefore, a single-layer of 40 wires equally distributed along the sides of the polygon is used to model the cross-section of the casing. The radius of each wire (0.99”, 2.5 cm) insures that the total transverse cross-section of the wires matches that of the casing.

Furthermore, the rapid decline of the transverse currents as a function of distance from the casing ends justifies the placement of denser wire loops near both ends of the casing than in the center portion of the casing. However, in order to maintain the same longitudinal cross-section of the casing, different conductor radii are selected as shown in Table 2. This table summarizes the data that was used to build the enhanced final model. Figure 6 illustrates the locations of wire’s radius assignment along the longitudinal (axial) direction of the casing.

Table 2. Location and Distribution of Wire’s Radius Assignment

Section No.	Length (feet)	Length (m)	Radius (feet)	Radius (m)	Total Number of Conductors in Each Section
1	5	1.524	0.086	0.026	10
2	5	1.524	0.122	0.037	5
3	10	3.048	0.173	0.053	5
4	20	6.096	0.273	0.083	4
5	60	18.288	0.300	0.091	10
6	20	6.096	0.273	0.083	4
7	10	3.048	0.173	0.053	5
8	5	1.524	0.122	0.037	5
9	5	1.524	0.086	0.026	10
<b>Total</b>	<b>140</b>	<b>43</b>			<b>58</b>

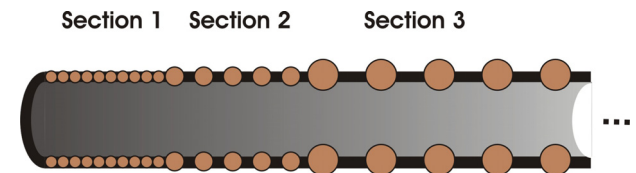


Figure 6. Locations of Wire’s Radius Assignment along the Longitudinal (Axial) Direction of the Casing

**4.2. Computation Results of Electromagnetic Model**

The electromagnetic field analysis was carried out for the various scenarios. The maximum average induced currents and its density along the longitudinal and transverse direction of the steel casing for the worst scenarios are displayed graphically in Figure 7 to 9.

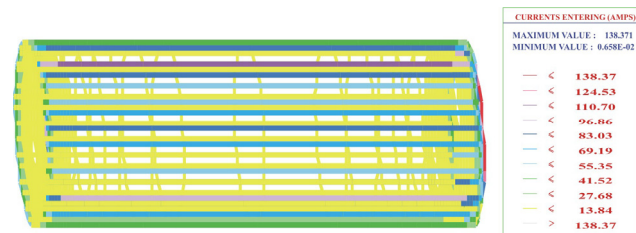


Figure 7. Average Current Distribution in the Casing

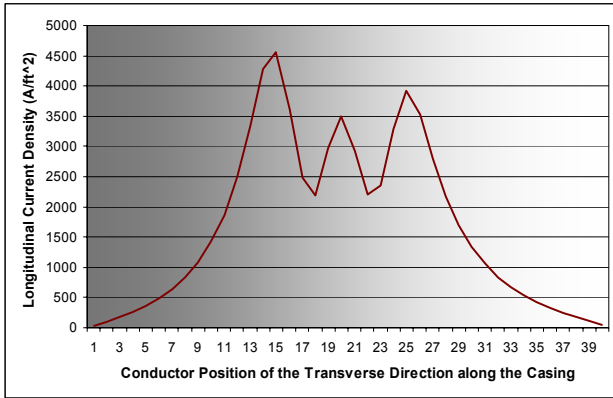


Figure 8. Average Current Density along Longitudinal Direction of the Casing

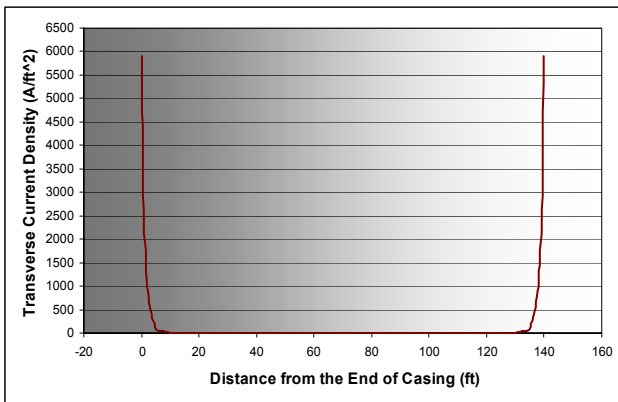


Figure 9. Average Current Density along the Transverse Direction of the Casing

The following information summarizes the computed induced currents in the casings based on the various scenarios:

- The induced currents flowing along the longitudinal (axial) direction of the casing are constant for each path and exhibit a peak when the path is closer to the energized phase conductor. On the other hand, the induced currents along the transverse (circular) direction are significant only near the ends of the steel casing and reach their peak at both ends of the 140' (43 m) casing.
- The highest density of induced current flowing along the longitudinal (axial) direction of the casings during emergency load cable operating condition is about 4556 A/foot<sup>2</sup> (49040 A/m<sup>2</sup>) with cross-bonding.
- The highest density of the induced currents flowing along the transverse (circular) directions on the casings during emergency load cable operating condition is 5903 A/foot<sup>2</sup> (63539 A/m<sup>2</sup>) with cross-bonding.

Let's assume that 4556 A/foot<sup>2</sup> (49040 A/m<sup>2</sup>) induced current flows in the casing (circulating loop current). The casing self impedance is 0.15775+j0.97354 ohm/mile based on the line parameter computations. The eddy current loss for a 1 foot (or 1 m) pipe casing section will be  $RI^2 = [0.3155/5280] 1950^2 = 227 \text{ W/foot (745 W/m)}$  (where R is the resistance of half the pipe casing, i.e.  $2[0.15775] = 0.3155$ ). The total cross-section of the casing is about 0.856 foot<sup>2</sup> (0.08 m<sup>2</sup>) and the current in that pipe portion is 4556  $[0.856 / 2] = 1950$ . This power loss due to the average eddy currents is unlikely to cause any significant heating as shown hereafter. Therefore, the exact current densities within the casing wall must be computed.

#### 4.3. Analytical Analysis

Note that two approximations have been made implicitly here. First, it is assumed that the currents flow in the pipe across two equal cross-sections and second, skin effects are accounted for in the calculation of the pipe casing resistance based on a unidirectional, perfectly symmetrical current flow along the pipe casing. The effects of these two approximations on the power loss calculation lead to optimistic conclusions as evidenced by the computation results shown in references [1, 2].

Skin effects (skin effect varies according to angular position), proximity effects (conductors close to the inner surface of the casing) and the circulating longitudinal current in the casing force the currents towards the inner surface and alter their paths. If the density of the current is significantly larger near the inner surface and along narrow paths then the eddy current losses will increase dramatically. Furthermore, the distribution of the electric field strength toward the interior and exterior surfaces when hysteresis is present results in an eddy current loss that is more than twice as large as when no hysteresis is present. Hysteresis also forces the current flow very near the surfaces. The skin depth is decreased largely. In addition, hysteresis losses that are not accounted for in the computations may represent up to 25% of the total losses in some adverse conditions [2].

Because of the importance of the various effects that distort the induced current paths on the conclusions that may be reached based on the computed current density magnitudes, the exact distribution of the induced casing currents in a cylindrical casing assuming no end effects (i.e., infinitely long cylinder) was computed analytically. This work was carried out based on the analytical equations described in [1, 2]. This work will be described in a separate paper along with the circuit model computation results.

The densities of the currents along the longitudinal and radial directions of the casing are shown in Figure 10 and Figure 11.

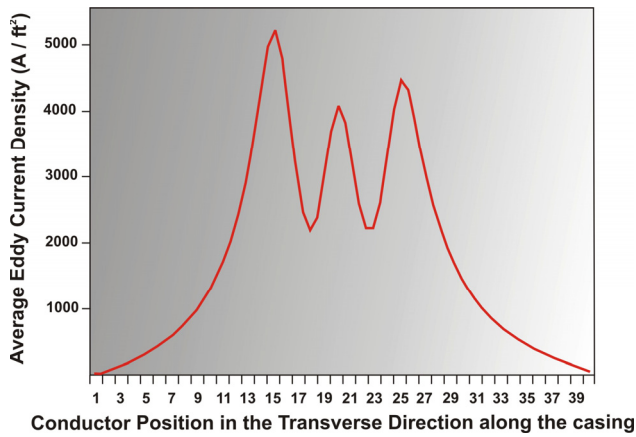


Figure 10. Average Current Densities along the Longitudinal Direction of the Casing

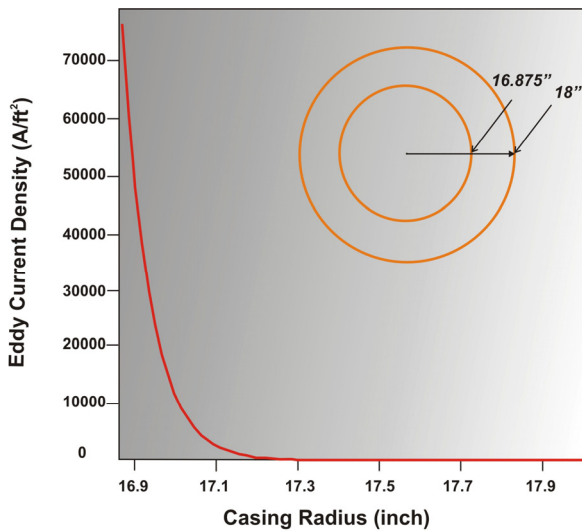


Figure 11. Current Densities along the Radial Direction of the Casing

There is a good agreement between the results computed using the analytical method and those obtained using the electromagnetic field computer model. The computed induced current flowing along the longitudinal direction of the casing is about 5282 A/foot<sup>2</sup> (56855 A/m<sup>2</sup>) near the conductor. Clearly, the current distribution is highly non-uniform, concentrating mainly in the first 1/4" (0.635 cm) of the casing thickness. The casing end effects are, of course, not accounted for in this model. However, this model reveals the dramatic proximity effect that forces most of the induced current to be restricted to less than 20% of the cross-section of the pipe casing. This phenomenon leads to a significant increase of the losses (up to 30 to 50 times more).

The total eddy current loss is computed by doing an integration of the eddy current loss over the cross-section of the steel casing.

$$P_e = \int_0^{2\pi} \int_{r_{inner}}^{r_{outer}} \rho_s |i(r, \varphi)|^2 r dr d\varphi$$

Where  $P_e$  is the eddy current loss.  $\rho_s$  is the relative resistivity of the steel casing,  $i$  is the eddy current,  $r_{outer}$  is the outer radius of the steel casing, and  $r_{inner}$  is the inner radius of the steel casing.

In summary, the computation results suggest that the eddy current losses can be enhanced by more than one order of magnitude due to the induced current path distortions. In the worst scenario, the estimated power loss is about 1910 W/foot (6266 W/m).

### 5. Conclusion

The contribution of the induced currents (eddy currents) in the steel casing of pipe-type cables to the heat losses in the casing were analyzed in detail based on the electromagnetic field theory. This study describes the approach used to determine the induced current distributions along the radial, transverse, and longitudinal directions of the casing taking into account the casing end effects. An analytical model of the cylindrical steel casing (assuming an infinitely long casing) was carried out to determine the current densities within the wall of the casing of the eddy currents induced along the steel casing.

The analysis shows clearly that induced currents within the pipe casing can cause significant heating in the casing at specific locations where the eddy current densities are enhanced by more than one order of magnitude due to end effects, proximity effects, and skin effects.

### 6. References

- [1] K. Kawasaki, M. Inami, T. Ishikawa, Theoretical Considerations on Eddy Current Losses in Non-Magnetic and Magnetic Pipes for Power Transmission Systems, Paper A 79 406-0, IEEE PES, Summer Meeting, Vancouver, BC, Canada, July 15-20, 1979.
- [2] C. W. McGee and Fred E. Vermeulen, Power Losses in Steel Pipe Delivering Very Large Currents, IEEE Transactions on Power Delivery, Vol. 17, No. 1, January 2002, pp25-32.
- [3] F. P. Dawalibi and F. Donoso, Integrated Analysis Software for Grounding, EMF, and EMI, IEEE Computer Applications in Power, 1993, Vol. 6, No. 2, pp. 19-24.
- [4] F. P. Dawalibi and A. Selby, Electromagnetic Fields of Energized Conductors, IEEE Transactions on Power Delivery, Vol. 8, No. 3, July 1993, pp. 1275-1284.